

# Model-driven gas exchange monitoring in the critically ill

Cosmin Balan<sup>1,2</sup>, Adrian View-Kim Wong<sup>1</sup>

<sup>1</sup>*Department of Critical Care Medicine, Oxford University Hospitals NHS Foundation Trust, John Radcliffe Hospital, United Kingdom*

<sup>2</sup>*Department of Anaesthesiology and Intensive Care Medicine, Bucharest Emergency University Hospital, Romania*

## Abstract

Understanding pulmonary gas exchange performance is a dynamic process which, depending on clinical context, exhibits different levels of complexity. Global tools such as tension-based indexes yield clinically crucial information under very specific conditions. Yet, accurate mechanistic insight can only originate in model-based tools. One-parameter models such as shunt or dead space are well established in clinical practice whilst two or three-parameter models have just been advanced and their role is yet to be delineated. Although the latter provide superior accuracy, this comes at the cost of increased complexity and possibly the need for invasive data sets. Modelling gas exchange enables a quantitative and physiologically-driven management of patients with lung failure. Assumptions are inherent to each tool and can clinically mislead if not accounted for. Thorough understanding of their subjacent theoretical construct is a prerequisite for their judicious use. This manuscript aims to describe current gas exchange monitoring tools, with special reference to their mathematical framework and constituent pitfalls. A unifying perspective on their clinical role is proposed.

Anaesthesiology Intensive Therapy 2018, vol. 50, no 2, 141–149

**Key words:** gas exchange, model; shunt; ventilation-perfusion mismatch; lung diffusion, dead space

Impaired respiratory function is common amongst critically ill patients; hence, insightful monitoring of gas exchange is paramount as it may translate into precise and objective therapeutic management.

Blood-gas relationships may be ascertained with a wide array of methods able to yield both qualitative and quantitative information, depending on clinical context. Outside the intensive care unit, clinicians may exhibit a “lumped” approach, such as merely reading system outputs (e.g. PaO<sub>2</sub>, SpO<sub>2</sub> or SaO<sub>2</sub>) or their interrelation to system input (e.g. PaO<sub>2</sub>/F<sub>i</sub>O<sub>2</sub>). Although this may suffice when facing simple clinical scenarios, its limits often push intensivists to favour mechanistic information derived from a system model approach. Shunt and dead space calculations are examples of classical one-parameter system models to address blood gas data, described as early as 1950 [1, 2]. These are well entrenched in current practice and capable of guiding an individualized hemodynamic and ventilator support; an interesting perspective on their use came from authors

investigating their ability to monitor the membrane lung [3]. Recently, two-parameter models have emerged as a more extensive method to identify and follow disturbances of pulmonary gas transfer. They dichotomize the oxygenation problem into shunt and a non-shunt compartment which is assigned to either diffusion limitation (R<sub>diff</sub>), alveolar dead space (V<sub>d</sub>alv) or ventilation-perfusion (V/Q) mismatch. Although superior as to performance to fit data when F<sub>i</sub>O<sub>2</sub> is varied, they have yet to become routine clinical practice tools.

All models come with caveats which are to be acknowledged in order to avoid seriously consequential pitfalls. Correct interpretation and bedside implementation of model-derived data warrants understanding of their underlying mathematical construct and its inherent assumptions.

## BASIC PRINCIPLES

This section aims to restate only those basic principles needed to allow a better understanding of the categorization and comparison of current tools to monitor pulmonary gas transfer.

Following a ubiquitous physiological principle such as mass conservation, a quantitative formulation of the ratio of alveolar ventilation to alveolar perfusion can be reached as previously described by Rahn and Riley [1, 2]:

$$VA/Q = (CcO_2 - CvO_2)/(F_iO_2 - FAO_2) \text{ (equation 1)}$$

where VA is alveolar ventilation; Q is total blood flow; Cc and Cv are pulmonary end-capillary and arterial blood concentrations; Fi and FA represent inspired and alveolar gas fractions; for simplicity, the Haldane transformation is neglected.

Diffusion, as stated by Fick, can be written as:

$$VO_2 = DLO_2 \cdot (PAO_2 - PcO_2) \text{ (equation 2)}$$

where DLO<sub>2</sub> is total diffusion capacity of O<sub>2</sub>, PA is alveolar pressure and Pc is pulmonary end-capillary blood concentration.

After converting fractions to pressures (FAO<sub>2</sub> = PAO<sub>2</sub> / (PB - PH<sub>2</sub>O) where PB is the barometric pressure and PH<sub>2</sub>O is water vapour pressure) and by combining equation 1 with 2, this gives:

$$VA/Q = (CcO_2 - CvO_2)/(F_iO_2 - (VO_2/DLO_2 + PcO_2)/(PB - PH_2O)) \text{ (equation 3)}$$

Equation 3 attests that main pulmonary factors modulating blood gas tensions (PcO<sub>2</sub>) are the range of V/Q ratios and the quality of the lung capillary barrier (DLO<sub>2</sub>). Extrapulmonary determinants represent another category subsumed in equation 3; total ventilation, haemoglobin (Hb), the composition of inspired gas and mixed venous blood, which in fact mirrors cardiac output and oxygen uptake, are the most relevant in daily practice [4]. Secondary extrapulmonary factors relate to the oxygen (ODC) and carbon dioxide (CO<sub>2</sub>DC) dissociating curves. Both categories can move in perfectly opposite directions such that lumped parameters like PaO<sub>2</sub> or PaO<sub>2</sub>/F<sub>i</sub>O<sub>2</sub> can be both inaccurate and misleading. Depending on the clinical context and chosen therapeutic strategy, it may become crucial to discern between the two types of factors (principle 1).

Although its position as a gold standard has been questioned, the multiple inert gases elimination technique (MIGET) remains the reference tool to describe pulmonary factors [5]. It allows diffusion impairment to be discarded as a common cause of hypoxemia leaving only the full V/Q spectrum to account for gas exchange disturbances in the critically ill population [6]. Thus, from a lung perspective, hypoxaemia and hypercapnia are best explained by shunt, dead space and V/Q mismatch, all parts of a continuum. Partitioning the contribution of

each mechanism would define the most comprehensive tool (principle 2).

## TENSION-BASED PARAMETERS

Tension-based indexes are first-order monitoring tools. Although they make useful adjuncts to any scoring system, they are essentially devoid of mechanistic insight and fail to meet the above-stated principles. Under special circumstances (see below), they may allow mechanistic information to be qualitatively deduced.

### 1. ALVEOLAR-ARTERIAL PO<sub>2</sub> (A-APO<sub>2</sub>)

The simplified alveolar gas equation corrects alveolar gas tensions for respiratory quotient and corresponding arterial tensions and serves to compute A-aPO<sub>2</sub>:

$$PAO_2 = P_iO_2 - PACO_2/R \text{ (equation 4)}$$

where P<sub>i</sub>O<sub>2</sub> is the O<sub>2</sub> pressure in the inspiratory gas, PACO<sub>2</sub> is the alveolar CO<sub>2</sub> pressure and R is the respiratory quotient. For simplicity, it is often assumed that PACO<sub>2</sub> is close to arterial CO<sub>2</sub> tension (PaCO<sub>2</sub>) but coexistent shunt invalidates this approximation [7].

A-aPO<sub>2</sub> was originally devised to distinguish hypoventilation-related hypoxemia from that elicited by a V/Q inequality or a diffusion limitation [8]. It was later shown to be fallible exactly under these circumstances; given that hypercapnia varies inversely with A-aPO<sub>2</sub>, a concomitant V/Q mismatch would tend to normalize this index and remain unaccounted for [9]. Meaningful yet qualitative information can be derived when F<sub>i</sub>O<sub>2</sub> is varied; with increasing F<sub>i</sub>O<sub>2</sub>, A-aPO<sub>2</sub> is expected to rise proportionately if shunt is prevalent whereas it will describe an inverted V shape if V/Q inequalities prevail [10].

### 2. PAO<sub>2</sub>/F<sub>i</sub>O<sub>2</sub>

PaO<sub>2</sub>/F<sub>i</sub>O<sub>2</sub> ratio is possibly the most popular tension-based tool to characterize gas exchange performance and a very strong predictor of mortality in the acute respiratory distress syndrome (ARDS). Its use is expected to extend outside critical care areas as arterial blood sampling is no longer obligatory for its determination. For peripheral oxygen saturations (SpO<sub>2</sub>) lying on the bend of the ODC, nonlinear computation of PaO<sub>2</sub>/F<sub>i</sub>O<sub>2</sub> from SpO<sub>2</sub>/F<sub>i</sub>O<sub>2</sub> [11] or mathematical conversion of venous oxygen tensions (PvO<sub>2</sub>) to arterial values (PaO<sub>2</sub>) [12] can circumvent the need to directly measure PaO<sub>2</sub>.

The amount of nonaerated lung can be tracked by the natural logarithm of PaO<sub>2</sub>/F<sub>i</sub>O<sub>2</sub> (lnPaO<sub>2</sub>/F<sub>i</sub>O<sub>2</sub>) obtained during pure oxygen ventilation [13]. Bedside estimation of end-expiratory lung volume (EELV) [14], or the delivered volume after a recruitment manoeuvre [15], are complementary methods to weigh the "baby lung" and launch a protective ventilation strategy.

Limitations of the  $P_{aO_2}/F_{iO_2}$  ratio mainly stem from its nonlinear behaviour when  $F_{iO_2}$  is varied. This relationship is actively and unpredictably modulated by the same intrapulmonary and extrapulmonary factors stated above, so that with fixed  $V/Q$  alterations an infinite number of  $P_{aO_2}/F_{iO_2}$  ratios becomes possible. A comprehensive mathematical formulation based on established gas transfer relations (see equation 7) has been derived [16] and simplifies to:

$$f(F_{iO_2}) = PaO_2 \text{ (equation 5)}$$

where  $f(F_{iO_2})$  comprises six physiological coefficients: PB,  $PaCO_2$ , R, Hb, S (shunt ratio), AVD (arterio-venous difference in oxygen content).

This translates the poor capacity of this index to specifically capture the magnitude of alveolo-capillary damage. Clinically, it is highly consequential as disease misclassification may ensue and cause treatment plans to neglect the true subjacent pathology [17].

## MODEL-BASED GAS EXCHANGE MONITORING

Gas exchange models merely approximate the real physiological picture. The ultimate test of model accuracy is its capacity to predict output (e.g.  $SaO_2$ ,  $SpO_2$  or expired fraction of  $O_2 - FeO_2$ ) from a given input (e.g.  $F_{iO_2}$ ) (principle 3). This also turns out to be a good measure of its comprehensiveness in that a tool obeying principle 2 cannot but satisfy principle 3.

Classical one-parameter models (physiological dead space, venous admixture/shunt) and research tools such as the multicompartamental MIGET are based on forward modelling theory whereby a system structure is assumed and behaviour is predicted. Monoparametrical models often fail to see inside the “black box” and provide a poor fit to measured data. On the contrary, MIGET meets all three enunciated principles and shows the best fit although complexity itself disqualifies it as a routine clinical procedure.

An inverse modelling approach, whereby the least complicated but essential system structure is inferred from input-output linkages, indicates that the minimum number of parameters needed to appropriately depict gas exchange is two [18]. Models revolving around two parameters, although far from encapsulating all details of gas transfer, provide the next best fit to patient data after MIGET.

A detailed mathematical description is beyond our scope and can be found elsewhere [19]; instead, best clinical use of available models will be emphasized with special reference to their theoretical framework.

### A. ONE-PARAMETER MODELS OF GAS EXCHANGE

In its simplest form, the oxygenation problem can be ascribed to a single cause: shunt, dead space,  $V/Q$  mismatch

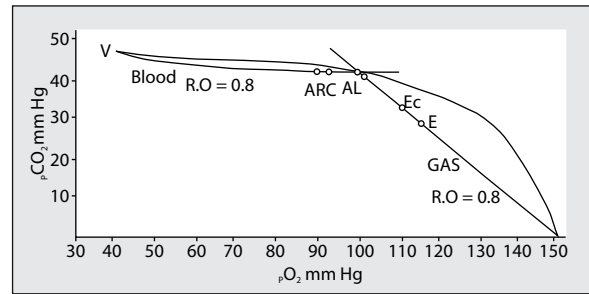


**Figure 1.** Classical  $O_2$ - $CO_2$  diagram showing all possible values for  $PO_2$  and  $PCO_2$  of alveoli with  $V/Q$  ranging from zero to infinity. Blood and gas R lines intersect in X. X — “ideal” alveolar air; C — mixed non-shunted alveolar capillary blood; AR — mixed arterial blood (after addition of shunt); AL — mixed alveolar air leaving all ventilated alveoli; E — mixed expired air; Ec — mixed expired air after correction for apparatus dead space; V — mixed venous blood; I — inspired air (reproduced with permission from Riley *et al.* [20])

or diffusion limitation. Each model only satisfies principle 1. Of these, the first two are most clinically relevant and represent second-order monitoring tools.

#### 1. SHUNT/VENOUS ADMIXTURE

Venous admixture may be thought of as the “alveolar dead space” of blood. It represents the deviation of arterial blood gas tensions towards mixed venous blood gas composition from that of an “ideal” alveolar blood-air interface which is defined by: 1) a local R equal to the respiratory quotient of the whole lung; and 2) a normal diffusion capacity (see Fig. 1) [20]. This “ideal” capillary-arterial gap is the result of alveoli with  $V/Q$  ratios less than “ideal” (lying at the left side of “X” in Fig. 1) and also includes true shunt ( $V/Q = 0$ ). As theoretically predicted, when present, diffusion problems augment the gap as well.

A conceptual model consists of two alveolar compartments of which one provides “ideal” gas exchange and the other completely lacks ventilation (see Fig. 2). After writing mass balance equations for blood flow and oxygen content, the classical shunt equation of Berggren can be readily arrived at:

$$\text{Shunt ratio } (S) = (CcO_2 - CaO_2) / (CcO_2 - CvO_2) \text{ (equation 6)}$$

Resolution of the term  $CcO_2$  requires the use of equation 4 and an ODC equation [21] to arrive at the corresponding pulmonary end-capillary saturation. Although computation of the denominator requires the use of a pulmonary artery catheter, this could be obviated by rewriting equation 6 and assuming a fixed AVD value (i.e.  $4.3 \text{ mL dl}^{-1}$ ) [20]. This approach is sensitive to cardiac output oscillations.

$$S/(1-S) = (CcO_2 - CaO_2) / AVD \text{ (equation 7)}$$

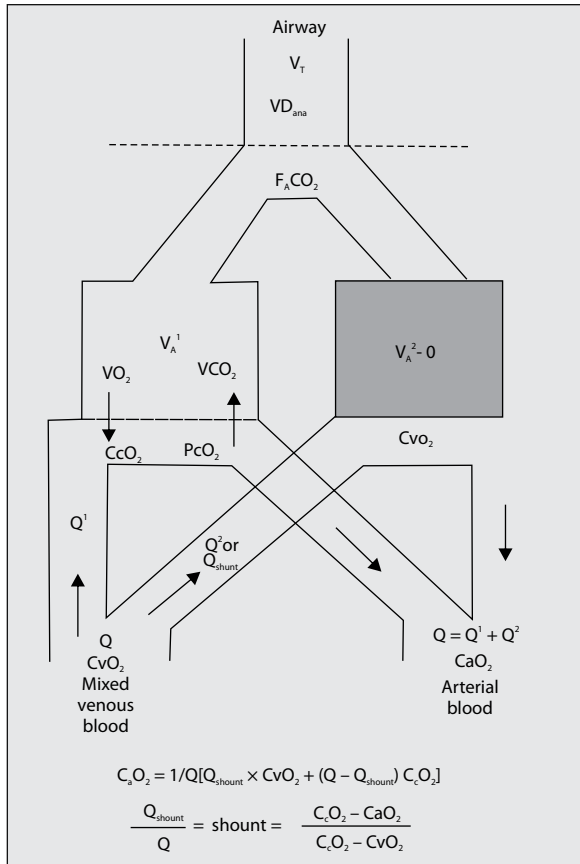


**Figure 2.** One-parameter, two-compartment model of shunt. Alveolar ventilation is absent in one compartment, leaving gas exchange to occur in the other one according to “ideal” conditions (see text for “ideal” definition). See Figure 5 for abbreviations

With increasing  $FIO_2$ ,  $V/Q$  inequalities wane and equation 6 will approximate true shunt. Any pure oxygen-related atelectasis may be successfully negated, or at least minimized, if sufficient positive end-expiratory pressure is already applied [22]. Measurement of shunt during 100% oxygen predicts the amount of nonaerated lung and becomes a useful bedside method to track recruitment/derecruitment episodes [13].

Computation of shunt is the most cited technique to characterize native and membrane lungs of patients on extracorporeal membrane oxygenation (ECMO) [3]. It has been successfully implemented in a mathematical model of oxygenation during veno-venous ECMO which can be accessed online ([www.ecmomodel.unimi.it](http://www.ecmomodel.unimi.it)) to help start up a preemptive therapeutic strategy [23].

**2. DEAD SPACE**

Similar to venous blood eluding gas exchange, air leaving non-perfused territories can be thought of as a “shunt”. Regardless of whether it originates in conducting airways ( $VD_{ana}$ ) or in alveoli ( $VD_{alv}$ ), dead space causes the compo-

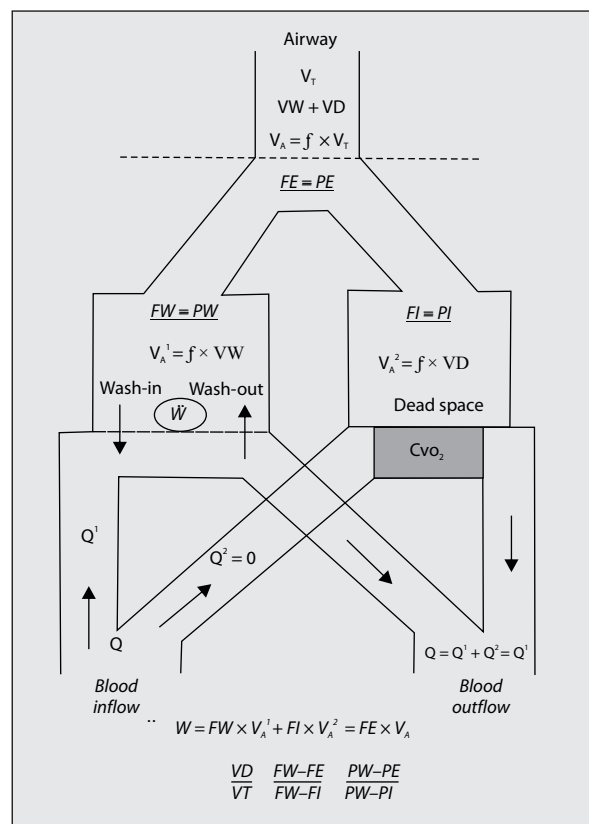


**Figure 3.** One-parameter, two-compartment model of dead space. Perfusion is absent in one compartment leaving gas exchange to occur in the other one according to “ideal” conditions.  $\dot{W}$  is the wash-in/wash-out rate of any tracer gas; FE, FW, FI are tracer gas fractions in mixed expiratory air, compartment W and the non-perfused compartment respectively. PE, PW, PI are corresponding pressures of the same tracer gas; equivalency of pressures with fractions is shown. VW, VD are tidal volumes of compartment W and dead space respectively. Breathing frequency is  $f$  and minute alveolar ventilation is shown in each compartment

sition of mixed alveolar air to diverge from that of an “ideal” compartment towards that of the inspired air (see Fig. 1).

Quantification of any dead space volume ( $VD$ ) can be reduced to a two compartment model analysis: a ventilated but non-perfused compartment and one capable of gas exchange ( $W$ ) (see Fig. 3). Mass balance relationships can be combined to obtain the following generalized formulation:

$$(PW - PE)/(PW - PI) = VD/(VD + VW) \text{ (equation 8)}$$

where any tracer gas is characterized by:  $PW$  as the partial pressure inside compartment  $W$ ;  $PE$  as the partial pressure in the mixed expired air flowing from both compartments;  $PI$  as the partial pressure in inspired air;  $VW$  is the volume of compartment  $W$ ; and  $VD$  is the volume of the non-perfused compartment ( $V/Q = \infty$ ). The absolute principle of this is that  $PW$  must only reflect the gas within  $W$  and cannot account for the gas within the dead space ( $V/Q = \infty$ ) (principle 4).

For the particular case of  $V_{Dana}$  and  $CO_2$  as a tracer gas, equation 8 becomes:

$$(P_{AmCO_2} - P_{ECO_2})/P_{AmCO_2} = V_{Dana}/VT \text{ (equation 9)}$$

where  $P_{AmCO_2}$  is the mean  $CO_2$  pressure of mixed alveolar air (approximated by end-tidal  $CO_2$  ( $P_{ETCO_2}$ ) if time-constants are perfectly homogeneous across the lung) and  $P_{ECO_2}$  is  $CO_2$  pressure of mixed expired air which can be derived from a volumetric capnogram ( $V_{cap}$ ) or classically measured with a Douglas bag;  $VT$  is tidal volume.

Being ascribed to Bohr, equation 9 conveys one very important message: mean  $CO_2$  pressure of all ventilated alveoli can only determine anatomical  $VD$ . Indeed, equation 9 was originally conceived to derive  $P_{AmCO_2}$  based on known  $V_{Dana}$  which had been measured on cadaver airways [24].

When compartment  $W$  is taken to represent an alveolar sector with "ideal" characteristics, equation 8 translates to the classical physiological dead space ( $VD_{phys}$ ) computation:

$$(P_{AiCO_2} - P_{ECO_2})/P_{AiCO_2} = VD_{phys}/VT \text{ (equation 10)}$$

where  $P_{AiCO_2}$  is the alveolar  $CO_2$  tension of an "ideal" territory as already defined.  $VD_{phys}$  will include not only anatomical dead space and true alveolar dead space ( $V/Q = \infty$ ) but also territories with  $V/Q$  values higher than "ideal" (lying at the right side of "X" in Fig. 1). Most confusion stems from defining  $P_{AiCO_2}$  as this will establish the  $V/Q$  range of what actually constitutes dead space.

Approximation of  $P_{AiCO_2}$  with  $P_{aCO_2}$  as originally suggested by Riley, is referred to as Enghoff's physiological dead space ( $VDe$ ).

$$(P_{aCO_2} - P_{ECO_2})/P_{aCO_2} = VDe/VT \text{ (equation 11)}$$

This is the favoured method to assess wasted ventilation and has recently been applied to artificial lungs as well [3]. Coexistent shunt, especially when larger than 40%, will erroneously elevate  $VDe$  [25]. This may turn out to be clinically useful when an inclusive index of lung state is called for as in prediction of mortality [26]. Dynamic monitoring of  $VDe$  detects lung collapse [27] and indicates the best positive end expiratory pressure (PEEP) [28] or the optimum inspiratory flow pattern [29]. On the contrary, a single value may not allow a differentiated ventilator strategy, as it may indicate both atelectasis and overdistension [30], each triggering a totally opposite action. Correction for shunt seems justified and has been achieved by several authors, with the most direct method provided by Kuwabara *et al.* [31]. As oxygen content is simplistically equated to oxygen pressures, the following results from equation 6:

$$P_{cCO_2} = P_{vCO_2} - [P_{vCO_2} - P_{aCO_2}/(1-S)] \text{ (equation 12)}$$

Concordant with Riley's model,  $P_{cCO_2}$  is taken to represent  $P_{AiCO_2}$  and thus equation 10 is combined with 12 to yield a corrected  $VD_{phys}$ .

Carbon dioxide kinetics will probably play an increasing role as a routine clinical decision tool with the advent of respiratory monitors capable of continuously tracking  $V_{cap}$ . With  $P_{aCO_2}$  superimposed on a  $CO_2$ - $VT$  plot, the graphical determination of  $VDe$  becomes possible and reproduces equation 11 [32]. The most common way to derive  $V_{Dana}$  is according to Fowler's equal area method which is, in fact, a geometrical representation of equation 9. In order to standardize  $V_{cap}$ , a mathematical function was recently applied to the raw  $CO_2$  waveform, allowing a more robust measurement of  $V_{Dana}$  and other curve specifics [33]. The same author group foregrounded the use of a mean alveolar  $CO_2$  pressure ( $P_{A_{BOHR}CO_2}$ ) to calculate "true" alveolar dead space ( $VD_{BOHR}$ ), uncontaminated by shunt effects [30]. It was commented that this approach merely equates to equation 9 [34]: using the mean of "all" alveoli as a substitute for  $P_W$  (see equation 8) will undoubtedly encapsulate units with high  $V/Q$  ratios (e.g.  $V/Q = \infty$ ) and therefore principle 4 is violated —  $VD_{alv}/VD_{phys}$  just cannot be inferred, only  $V_{Dana}$  can. This contrasts with the proven ability of  $VD_{BOHR}$  to actually track  $VD_{alv}$  in a cardiac surgery patient [34], or detect overdistension during a PEEP trial [35]. To clarify this discrepancy, it is useful to consider the proposed determination of the "airway-alveolar" interface which is different from Fowler's method. As the authors clearly show, under most circumstances, Fowler's method will underestimate the  $V_{Dana}$  calculated by their method [33]. The net result is that  $P_{A_{BOHR}CO_2}$  will lie at the right side of  $P_{AmCO_2}$ , which is closer to a virtual  $P_{AiCO_2}$  (i.e.  $P_{aCO_2}$  according to Riley). Conveniently, this means that, under most circumstances,  $P_{A_{BOHR}CO_2}$  will not be the "true mean" as it fails to represent all alveoli and  $VD_{BOHR}$  will then be able to capture  $VD_{alv}$ .

Measured together,  $VDe$  and  $VD_{BOHR}$  cover the entire continuum of  $V/Q$  ratios, provide complementary data and can act in concert to enable a lung-protective ventilatory strategy.

Lastly, the information obtained from  $V_{cap}$  could extend beyond the assessment of  $CO_2$  volumes. Waveform morphology distorts specifically with alveolar recruitment and reflects acinar gas mixing and perfusion [36, 37]. The translatability of these findings into clinical practice is yet awaited.

## B. TWO-PARAMETER MODELS OF GAS EXCHANGE

These are third-order tools to monitor pulmonary gas exchange as they meet both principles 1 and 3. Their conceptualization originates in Riley's work (see Fig. 1) [20]. Between ideal capillary and arterial blood, two virtual oxygen gaps can be delineated: one caused by "pure" shunt (distance between AR and C) and a second represented by

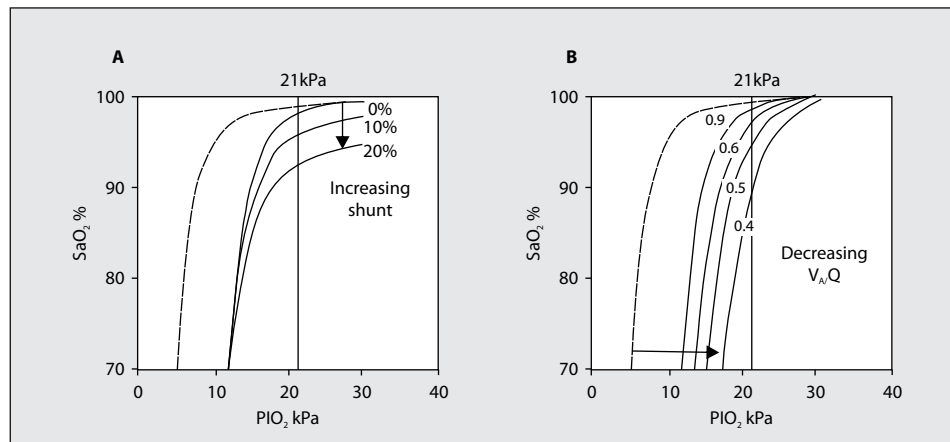


**Figure 4.** Effects of increasing shunt or reducing ventilation — perfusion (V/Q) ratio on a plot of  $PiO_2$  versus  $SaO_2$ . The dashed line identifies the oxygen dissociation curve (reproduced with permission from Rowe *et al.* [39])

the difference between ideal capillary and mixed capillary blood ( $\Delta PO_2$  is distance from X to C). The latter could be attributed to either  $R_{diff}$ , V/Q mismatch (any  $V/Q > 0$ ) or a mixture of these but, with  $R_{diff}$  cast off as a common cause of hypoxemia in the critically ill (see above),  $\Delta PO_2$  can be entirely attributed to the V/Q state.

Shunt and  $\Delta PO_2$  are embedded in plots of  $PiO_2$  versus  $SpO_2$  such that, after adjustment for their effect and correction for alveolar air (equation 4), complete identity between ODC and the  $PiO_2 - SpO_2$  diagram is mathematically demonstrable [38]. An increasing shunt will produce a specific downward shift of the original ODC whereas  $\Delta PO_2$  relates to a rightward displacement of the curve (see Fig. 4); ultimately, a unique  $PiO_2 - SpO_2$  plot inclosing all synchronous gas exchange abnormalities is ready to be deciphered.

The first mathematical formulation of these models was generated by Sapsford and Jones.<sup>38</sup> Simplistically, it can be restated as:

$$f(PiO_2) = f(PiO_2) = SaO_2 \text{ (equation 13)}$$

where  $f(PiO_2)$  comprises two unknowns (shunt and  $\Delta PO_2$ ) and several physiological coefficients of which haemoglobin and cardiac output result in the largest sensitivity. Correct identification of system parameters requires at least two  $PiO_2/SaO_2$  data sets which should range over the maximal downward curvature of the  $PiO_2 - SpO_2$  plot to ensure optimum model fit (i.e. close to  $SaO_2/SpO_2$  of 96%) [40]. The implicit assumption hereof is that multiple  $F_iO_2$  steps will not alter lung physiology; this may be valid only as long as an upper limit of 0.8 is respected [41].

A refinement came from Kjaergaard *et al.* [19] who advanced a three-compartment, two-parameter model (see Fig. 5). Data sets belong to a plot of  $F_eO_2$  versus  $SpO_2/SaO_2$ . A fixed perfusion split ( $f_2 = 0.9$ ) is assigned to the non-shunted

blood serving two alveolar compartments ventilated according to a variable fraction ( $fA_2$ ) which indirectly becomes a measure of V/Q heterogeneity. Optimum gas exchange is simulated at zero shunt and  $fA_2$  equal to 0.9 ( $\Delta PO_2 = 0kPa$ ). Although far from fulfilling principle 2, this “minimal” model fits with acceptable accuracy MIGET data sets [42] and significantly outperforms one-parameter models (i.e. shunt in equation 7 or 5) in predicting the  $PaO_2/FiO_2$  behaviour to varying  $F_iO_2$  [17]. Improved accuracy, but at the cost of increased complexity, comes with the addition of a third free parameter ( $f_2$  as the fractional perfusion distributor) and the writing of alveolar and blood mass balance equations for both  $O_2$  and  $CO_2$  [43].

Clinical use is yet to be defined. Non-invasive determination of parameters will probably enable wider application of these models [44], as will the free distribution of simple, intuitive bedside tools (<http://www.noranaes.org/shuntcurves/>).

Failure to differentiate between shunt and V/Q mismatch precludes a flexible and advised therapy. Such a dichotomized view has been shown to inform on the risk of post-operative hypoxemia, the impact of anticongestive therapy, lung recruitability or PEEP selection and could be envisaged to assess any drug-related (e.g. nitric oxide) or mechanically-induced V/Q alteration [19, 45, 46]. “Minimal” models of gas exchange have been assimilated to advanced model-based decision supports, such as the Intelligent Ventilator (INVENT) project [47] or non-invasive cardiac output estimators [48]. In addition, because a stepwise variation in  $F_iO_2$  simply imitates a tracer gas (oxygen as in Weissman’s LUFU system [49], or nitrogen as described by Stenqvist *et al.* [50]), functional residual capacity (FRC) or EELV would be readily attainable and overall lung strain may be calculated from sequential EELV determinations [14]. The extent of local inhomogeneities is imprinted in oxygen washout curves which could provide yet another useful index [51]. Overall,

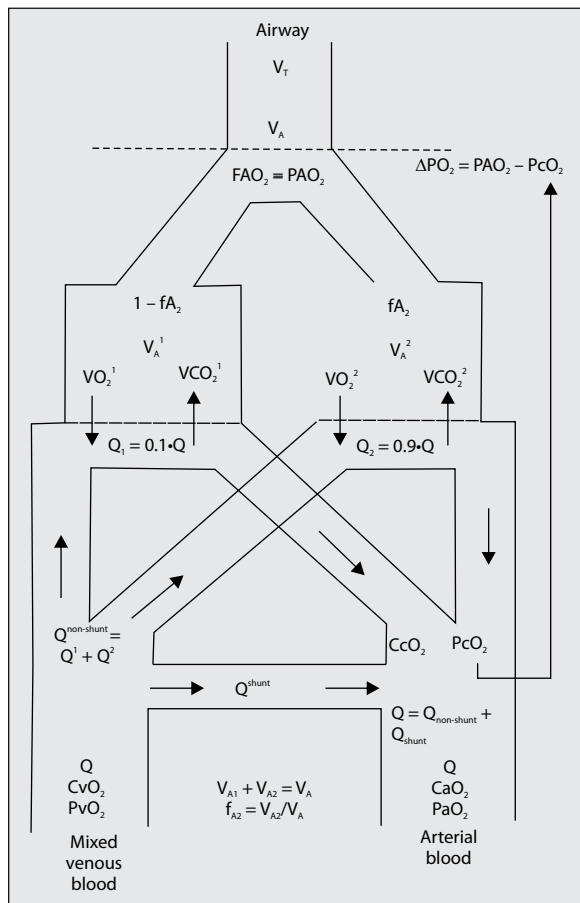


**Figure 5.** Minimal model of gas exchange with three compartments and two parameters: a pulmonary shunt compartment and two others ventilated according to a fractional ventilation distributor ( $f_{A_2}$ ).  $V_A$  — alveolar ventilation;  $V_A^1$  and  $V_A^2$  — alveolar ventilation of the ventilated compartments;  $Q$  — overall cardiac output;  $PvO_2$  — mixed venous pressure of oxygen;  $CvO_2$  — oxygen content in mixed venous blood;  $PaO_2$  — systemic arterial pressure of oxygen;  $CaO_2$  — oxygen content in systemic arterial blood;  $Q^{shunt}$  — shunted venous blood flow;  $Q^1$  and  $Q^2$  — blood flows corresponding to ventilated compartments;  $PcO_2$  — non-shunted end-capillary oxygen pressure;  $CcO_2$  — oxygen content in non-shunted end-capillary blood;  $PAO_2$  — mixed alveolar air oxygen pressure;  $VO_2^{1,2}$  and  $VCO_2^{1,2}$  compartmental  $O_2$  consumption and  $CO_2$  production respectively (adapted after Karbing *et al.* [42])

a simple bedside manoeuvre such as  $FiO_2$  variation could coordinate a highly personalized, physiologically-oriented stress-free ventilation strategy.

## DISCUSSION

Deciding which monitoring test to use is clinically consequential. It is tempting to define the ideal tool as that which offers the most exhaustive description of gas exchange. MIGET could then emerge as the ultimate choice were it not for its cumbersome and costly preparation. Hierarchically, three-parameter models followed by two-parameter models would come next. Could these be the optimum tools to monitor pulmonary gas exchange?

Critical illness offers a diverse array of challenges, ranging from a simple dichotomous decision of whether to turn prone an ARDS patient to a dynamic, quantitative assessment of lung state following a change in ventilator settings. Physicians will face situations which call for a pragmatic and undifferentiated approach devised to set out a timely therapeutic plan. The necessity for a low tidal volume strategy should rely on the clinical context and elementary tools such as the  $PaO_2/FiO_2$  ratio. Likewise, Enghoff's  $VD$  may serve as a very strong predictor of mortality in ARDS patients and this is probably due to its global nature resulting from the failure to separate shunt from dead space. An accurate split-view of these two mechanisms may turn out to be advantageous when an informed open lung strategy is considered. The solution thereof is a combination of  $VD_{BOHR}$  and the computation of equation 6 during a short episode of pure oxygen ventilation. Alternatively, discriminating between shunt and  $V/Q$  imbalance with third-order monitoring tools may generate an even more inclusive and reproducible picture, one closer to patient physiology and remarkably accurate when set against MIGET.

Thus, it appears that appropriateness in context may be the correct descriptor of the ideal tool. If weighed carefully, clinical settings will advise one of the right balance between the information yield and the complexity of a test. An optimum, but often different monitoring method will then ensue within each clinical scenario. To answer the question above, any tool may be ideal but only when used in the right context.

## CONCLUSION

Model-based quantification of pulmonary gas exchange merely approximates the complexity of real physiological processes. If limits inherent to their underlying mathematical construct are thoroughly acknowledged, these tools enable rational, uniform and physiologically-oriented clinical decision making. Optimum use rests in each clinician's ability to tune the right model to the appropriate context and patient in a timely fashion.

## ACKNOWLEDGEMENTS

1. Source of funding: none.
2. Conflict of interest: none.

## References:

1. Rahn H, Fenn WO. A graphical analysis of the respiratory gas exchange; the Ob2-CO2 diagram. Washington: American Physiological Society. 1955.
2. Riley RL, Courand A. Analysis of factors affecting partial pressures of oxygen and carbon dioxide in gas and blood of lungs; theory. *J Appl Physiol.* 1951; 4(2): 77–101, indexed in Pubmed: [14888620](https://pubmed.ncbi.nlm.nih.gov/14888620/).
3. Zanella A, Mojoli F, Castagna L, Patroniti N. Respiratory monitoring of the ECMO patient. In: Sangalli F, Patroniti N, Pesenti A. ed. *ECMO-Extracorporeal life support in adults*. Springer Milan, Milano 214: 249–263.

4. Rodriguez-Roisin R, Roca J, Barbera JA. Extrapulmonary and Intrapulmonary Determinants of Pulmonary Gas Exchange. *Ventilatory Failure*. 1991; 18–36, doi: [10.1007/978-3-642-84554-3\\_2](https://doi.org/10.1007/978-3-642-84554-3_2).
5. Olszowka AJ. Can VA/Q distributions in the lung be recovered from inert gas retention data? *Respir Physiol*. 1975; 25(2): 191–198, indexed in Pubmed: [173002](https://pubmed.ncbi.nlm.nih.gov/173002/).
6. Hedenstierna G, Gunnarsson L. Ventilation-perfusion distribution and diffusion limitations. oxygen transport in the critically ill patient. 1990; 7–16, doi: [10.1007/978-3-642-75646-7\\_2](https://doi.org/10.1007/978-3-642-75646-7_2).
7. Cruickshank S, Hirschauer N. The alveolar gas equation. *Continuing Education in Anaesthesia, Critical Care & Pain*. 2004; 4(1): 24–27, doi: [10.1093/bjaceaccp/mkh008](https://doi.org/10.1093/bjaceaccp/mkh008).
8. FARHI LE, RAHN H. A theoretical analysis of the alveolar-arterial O<sub>2</sub> difference with special reference to the distribution effect. *J Appl Physiol*. 1955; 7(6): 699–703, indexed in Pubmed: [14381350](https://pubmed.ncbi.nlm.nih.gov/14381350/).
9. Gray BA, Blalock JM. Interpretation of the alveolar-arterial oxygen difference in patients with hypercapnia. *Am Rev Respir Dis*. 1991; 143(1): 4–8, doi: [10.1164/ajrccm/143.1.4](https://doi.org/10.1164/ajrccm/143.1.4), indexed in Pubmed: [1898845](https://pubmed.ncbi.nlm.nih.gov/1898845/).
10. Peter DW. *Textbook of Critical Care*. Oxford 2016.
11. Brown SM, Grissom CK, Moss M, et al. NIH/NHLBI PETAL Network Collaborators. Nonlinear imputation of PaO<sub>2</sub>/Fio<sub>2</sub> from SpO<sub>2</sub>/Fio<sub>2</sub> among patients with acute respiratory distress syndrome. *Chest*. 2016; 150(2): 307–313, doi: [10.1016/j.chest.2016.01.003](https://doi.org/10.1016/j.chest.2016.01.003), indexed in Pubmed: [26836924](https://pubmed.ncbi.nlm.nih.gov/26836924/).
12. Toftegaard M, Rees SE, Andreassen S. Evaluation of a method for converting venous values of acid-base and oxygenation status to arterial values. *Emerg Med J*. 2009; 26(4): 268–272, doi: [10.1136/emj.2007.052571](https://doi.org/10.1136/emj.2007.052571), indexed in Pubmed: [19307387](https://pubmed.ncbi.nlm.nih.gov/19307387/).
13. Reske AW, Costa ELV, Reske AP, et al. Bedside estimation of nonaerated lung tissue using blood gas analysis. *Crit Care Med*. 2013; 41(3): 732–743, doi: [10.1097/CCM.0b013e3182711b6e](https://doi.org/10.1097/CCM.0b013e3182711b6e), indexed in Pubmed: [23318487](https://pubmed.ncbi.nlm.nih.gov/23318487/).
14. Blankman P, Hasan D, Bikker IG, et al. Lung stress and strain calculations in mechanically ventilated patients in the intensive care unit. *Acta Anaesthesiol Scand*. 2016; 60(1): 69–78, doi: [10.1111/aas.12589](https://doi.org/10.1111/aas.12589), indexed in Pubmed: [26192561](https://pubmed.ncbi.nlm.nih.gov/26192561/).
15. Beitler JR, Majumdar R, Hubmayr RD, et al. Volume delivered during recruitment maneuver predicts lung stress in acute respiratory distress syndrome. *Crit Care Med*. 2016; 44(1): 91–99, doi: [10.1097/CCM.0000000000001355](https://doi.org/10.1097/CCM.0000000000001355), indexed in Pubmed: [26474111](https://pubmed.ncbi.nlm.nih.gov/26474111/).
16. Aboab J, Louis B, Jonson B, Brochard L. Relation between PaO<sub>2</sub>/Fio<sub>2</sub> ratio and FIO<sub>2</sub>: a mathematical description. In: Pinsky MR, Brochard L, Mancebo J. ed. *Applied physiology in intensive care medicine*. Springer Berlin Heidelberg, Berlin, Heidelberg 2006: 41–44.
17. Karbing DS, Kjaergaard S, Smith BW, et al. Variation in the PaO<sub>2</sub>/Fio<sub>2</sub> ratio with FIO<sub>2</sub>: mathematical and experimental description, and clinical relevance. *Crit Care*. 2007; 11(6): R118, doi: [10.1186/cc6174](https://doi.org/10.1186/cc6174), indexed in Pubmed: [17988390](https://pubmed.ncbi.nlm.nih.gov/17988390/).
18. Mathematical modelling of pulmonary gas exchange. In: Karbing DS, Carson E, Cobelli C. ed. *Modelling methodology for physiology and medicine*, 2nd ed. Elsevier, Inc. 2014: 281–309.
19. Kjaergaard SC. *Mathematical models of pulmonary gas exchange — validation and application to postoperative hypoxaemia*. PhD Thesis. Aalborg University 2003.
20. Riley RL, Courand A. Ideal alveolar air and the analysis of ventilation-perfusion relationships in the lungs. *J Appl Physiol*. 1949; 1(12): 825–847, indexed in Pubmed: [18145478](https://pubmed.ncbi.nlm.nih.gov/18145478/).
21. Dash RK, Bassingthwaighe JB, Dash RK, et al. Blood HbO<sub>2</sub> and HbCO<sub>2</sub> dissociation curves at varied O<sub>2</sub>, CO<sub>2</sub>, pH, 2,3-DPG and temperature levels. *Ann Biomed Eng*. 2004; 32(12): 1676–1693, indexed in Pubmed: [15682524](https://pubmed.ncbi.nlm.nih.gov/15682524/).
22. Aboab J, Jonson B, Kouatchet A, et al. Effect of inspired oxygen fraction on alveolar derecruitment in acute respiratory distress syndrome. *Intensive Care Med*. 2006; 32(12): 1979–1986, doi: [10.1007/s00134-006-0382-4](https://doi.org/10.1007/s00134-006-0382-4), indexed in Pubmed: [17019545](https://pubmed.ncbi.nlm.nih.gov/17019545/).
23. Zanella A, Salerno D, Scaravilli V, et al. A mathematical model of oxygenation during venovenous extracorporeal membrane oxygenation support. *J Crit Care*. 2016; 36: 178–186, doi: [10.1016/j.jccr.2016.07.008](https://doi.org/10.1016/j.jccr.2016.07.008), indexed in Pubmed: [27546769](https://pubmed.ncbi.nlm.nih.gov/27546769/).
24. Lumb AB. *Nunn's applied respiratory physiology*. Elsevier 2017: 122–123.
25. Niklason L, Eckerström J, Jonson B. The influence of venous admixture on alveolar dead space and carbon dioxide exchange in acute respiratory distress syndrome: computer modelling. *Crit Care*. 2008; 12(2): R53, doi: [10.1186/cc6872](https://doi.org/10.1186/cc6872), indexed in Pubmed: [18423016](https://pubmed.ncbi.nlm.nih.gov/18423016/).
26. Nuckton TJ, Alonso JA, Kallet RH, et al. Pulmonary dead-space fraction as a risk factor for death in the acute respiratory distress syndrome. *N Engl J Med*. 2002; 346(17): 1281–1286, doi: [10.1056/NEJMoa012835](https://doi.org/10.1056/NEJMoa012835), indexed in Pubmed: [11973365](https://pubmed.ncbi.nlm.nih.gov/11973365/).
27. Tusman G, Suarez-Sipmann F, Böhm SH, et al. Monitoring dead space during recruitment and PEEP titration in an experimental model. *Intensive Care Med*. 2006; 32(11): 1863–1871, doi: [10.1007/s00134-006-0371-7](https://doi.org/10.1007/s00134-006-0371-7), indexed in Pubmed: [17047925](https://pubmed.ncbi.nlm.nih.gov/17047925/).
28. Maisch S, Reissmann H, Fuellekrug B, et al. Compliance and dead space fraction indicate an optimal level of positive end-expiratory pressure after recruitment in anesthetized patients. *Anesth Analg*. 2008; 106(1): 175–81, table of contents, doi: [10.1213/01.ane.0000287684.74505.49](https://doi.org/10.1213/01.ane.0000287684.74505.49), indexed in Pubmed: [18165575](https://pubmed.ncbi.nlm.nih.gov/18165575/).
29. Aboab J, Niklason L, Uttman L, et al. Dead space and CO<sub>2</sub> elimination related to pattern of inspiratory gas delivery in ARDS patients. *Crit Care*. 2012; 16(2): R39, doi: [10.1186/cc11232](https://doi.org/10.1186/cc11232), indexed in Pubmed: [22390777](https://pubmed.ncbi.nlm.nih.gov/22390777/).
30. Tusman G, Sipmann FS, Böhm SH. Rationale of dead space measurement by volumetric capnography. *Anesth Analg*. 2012; 114(4): 866–874, doi: [10.1213/ANE.0b013e318247f6cc](https://doi.org/10.1213/ANE.0b013e318247f6cc), indexed in Pubmed: [22383673](https://pubmed.ncbi.nlm.nih.gov/22383673/).
31. Kuwabara S, Duncalf D. Effect of anatomic shunt on physiologic dead-space-to-tidal volume ratio—a new equation. *Anesthesiology*. 1969; 31(6): 575–577, indexed in Pubmed: [5348825](https://pubmed.ncbi.nlm.nih.gov/5348825/).
32. Tang Y, Turner MJ, Baker AB. A new equal area method to calculate and represent physiologic, anatomical, and alveolar dead spaces. *Anesthesiology*. 2006; 104(4): 696–700, indexed in Pubmed: [16571964](https://pubmed.ncbi.nlm.nih.gov/16571964/).
33. Tusman G, Scandurra A, Böhm SH, et al. Model fitting of volumetric capnograms improves calculations of airway dead space and slope of phase III. *J Clin Monit Comput*. 2009; 23(4): 197–206, doi: [10.1007/s10877-009-9182-z](https://doi.org/10.1007/s10877-009-9182-z), indexed in Pubmed: [19517259](https://pubmed.ncbi.nlm.nih.gov/19517259/).
34. Graf J. Comment on Tusman et al.: Validation of Bohr dead space measured by volumetric capnography. *Intensive Care Med*. 2011; 37(8): 1396, doi: [10.1007/s00134-011-2280-7](https://doi.org/10.1007/s00134-011-2280-7), indexed in Pubmed: [21713560](https://pubmed.ncbi.nlm.nih.gov/21713560/).
35. Suarez-Sipmann FSA, Tusman G, Böhm SH, et al. Bohr's dead space helps to detect overdistension during a PEEP trial. *Devices and monitoring in intensive care unit*. 2012: A3777-A.
36. Suarez-Sipmann F, Tusman G, Böhm SH. Volumetric capnography for monitoring lung function during mechanical ventilation. *Intensive Care Medicine*. : 458–467, doi: [10.1007/0-387-35096-9\\_42](https://doi.org/10.1007/0-387-35096-9_42).
37. Tusman G, Areta M, Climente C, et al. Effect of pulmonary perfusion on the slopes of single-breath test of CO<sub>2</sub>. *J Appl Physiol* (1985). 2005; 99(2): 650–655, doi: [10.1152/jappphysiol.01115.2004](https://doi.org/10.1152/jappphysiol.01115.2004), indexed in Pubmed: [15802365](https://pubmed.ncbi.nlm.nih.gov/15802365/).
38. Sapsford DJ, Jones JG. The P<sub>IO</sub><sub>2</sub> vs. SpO<sub>2</sub> diagram: a non-invasive measure of pulmonary oxygen exchange. *Eur J Anaesthesiol*. 1995; 12(4): 375–386, indexed in Pubmed: [7588667](https://pubmed.ncbi.nlm.nih.gov/7588667/).
39. Rowe L, Jones JG, Quine D, et al. A simplified method for deriving shunt and reduced VA/Q in infants. *Arch Dis Child Fetal Neonatal Ed*. 2010; 95(1): F47–F52, doi: [10.1136/adc.2009.160010](https://doi.org/10.1136/adc.2009.160010), indexed in Pubmed: [19700395](https://pubmed.ncbi.nlm.nih.gov/19700395/).
40. Riedlinger A, Kretschmer J, Möller K. Estimating the measuring effort for using a two-parameter gas exchange model in clinical practice. *IFAC Proceedings Volumes*. 2014; 47(3): 9886–9889, doi: [10.3182/20140824-6-za-1003.02146](https://doi.org/10.3182/20140824-6-za-1003.02146).
41. Edmark L, Kostova-Aherdan K, Enlund M, et al. Optimal oxygen concentration during induction of general anesthesia. *Anesthesiology*. 2003; 98(1): 28–33, indexed in Pubmed: [12502975](https://pubmed.ncbi.nlm.nih.gov/12502975/).
42. Rees SE, Kjaergaard S, Andreassen S, et al. Reproduction of MIGET retention and excretion data using a simple mathematical model of gas exchange in lung damage caused by oleic acid infusion. *J Appl Physiol* (1985). 2006; 101(3): 826–832, doi: [10.1152/jappphysiol.01481.2005](https://doi.org/10.1152/jappphysiol.01481.2005), indexed in Pubmed: [16763097](https://pubmed.ncbi.nlm.nih.gov/16763097/).
43. Karbing DS, Kjaergaard S, Andreassen S, et al. Minimal model quantification of pulmonary gas exchange in intensive care patients. *Med Eng Phys*. 2011; 33(2): 240–248, doi: [10.1016/j.medengphy.2010.10.007](https://doi.org/10.1016/j.medengphy.2010.10.007), indexed in Pubmed: [21050794](https://pubmed.ncbi.nlm.nih.gov/21050794/).
44. Kjaergaard S, Rees S, Malczynski J, et al. Non-invasive estimation of shunt and ventilation-perfusion mismatch. *Intensive Care Med*. 2003; 29(5): 727–734, doi: [10.1007/s00134-003-1708-0](https://doi.org/10.1007/s00134-003-1708-0), indexed in Pubmed: [12698242](https://pubmed.ncbi.nlm.nih.gov/12698242/).
45. Moesgaard J, Kristensen JH, Malczynski J, et al. Can new pulmonary gas exchange parameters contribute to evaluation of pulmonary congestion in left-sided heart failure? *Can J Cardiol*. 2009; 25(3): 149–155, indexed in Pubmed: [19279982](https://pubmed.ncbi.nlm.nih.gov/19279982/).
46. Jones JG, Jones SE. Discriminating between the effect of shunt and reduced VA/Q on arterial oxygen saturation is particularly useful in

- clinical practice. *J Clin Monit Comput.* 2000; 16(5-6): 337–350, indexed in Pubmed: [12580217](#).
47. Rees SE. The Intelligent Ventilator (INVENT) project: the role of mathematical models in translating physiological knowledge into clinical practice. *Comput Methods Programs Biomed.* 2011; 104 Suppl 1: S1–29, doi: [10.1016/S0169-2607\(11\)00307-5](#), indexed in Pubmed: [22152752](#).
48. Sundaresan A, Chase JG, Hann CE, et al. Cardiac output estimation using pulmonary mechanics in mechanically ventilated patients. *Biomed Eng Online.* 2010; 9: 80, doi: [10.1186/1475-925X-9-80](#), indexed in Pubmed: [21108836](#).
49. Weismann D, Reissmann H, Maisch S, et al. Monitoring of functional residual capacity by an oxygen washin/washout; technical description and evaluation. *J Clin Monit Comput.* 2006; 20(4): 251–260, doi: [10.1007/s10877-006-9029-9](#), indexed in Pubmed: [16832581](#).
50. Olegård C, Söndergaard S, Houltz E, et al. Estimation of functional residual capacity at the bedside using standard monitoring equipment: a modified nitrogen washout/washin technique requiring a small change of the inspired oxygen fraction. *Anesth Analg.* 2005; 101(1): 206–12, table of contents, doi: [10.1213/01.ANE.0000165823.90368.55](#), indexed in Pubmed: [15976233](#).
51. Bikker IG, Holland W, Specht P, et al. Assessment of ventilation inhomogeneity during mechanical ventilation using a rapid-response oxygen sensor-based oxygen washout method. *Intensive Care Med Exp.* 2014; 2(1): 14, doi: [10.1186/2197-425X-2-14](#), indexed in Pubmed: [26266910](#).

**Corresponding author:**

*Cosmin Balan*  
*Porumbacu Street*  
*Flat 89, Bucharest 060366, Romania*  
*e-mail: cosmin13mara@yahoo.com*

*Received: 23.09.2017*

*Accepted: 11.11.2017*